Computer Aided Modeling of Fiber Assemblies

Keartisak Sreprateep[1] and Erik L. J. Bohez[2]

[1]Asian Institute of Technology, Keartisak.Sreprateep@ait.ac.th
[2]Asian Institute of Technology, bohez@ait.ac.th

ABSTRACT

An algorithm of 3D modeling of fibers assemblies has been developed. The method extends a concept of 'virtual location' for simulation of fiber distributions in yarns cross-section from 2D to 3D modeling of yarns structure. The distributions function used in the model demonstrates all of the properties of the ideal and real yarns. A series of further cross-section at equal intervals along the yarn length is given. Each cross-section is rotated by a pre-determined amount relative to previous one, to allow for the yarn twist and parameters of fibers migration. The fiber curve in each interval between two successive cross-sections is approximated by NURBS. Also curve generation based on twist of each fiber is determined by centerline configurations of their constituent fibers and the generative model. Each fiber is created by sweeping a closed curve along a centerline path. The simulated yarns structure using the algorithm described can model wider variety and yield an improved visual representation of real yarn structure.

Keywords: Fibers assemblies, CAD/CAE, Textile, Yarns structure

1. INTRODUCTION

The two primary features of textile are the geometric complexity of most textile structure and the anisotropy, nonlinear behavior of many fibers. The response of fibers assemblies to an applied mechanical load is dominated by fiber to fiber interactions. Beyond this, there was, and still is the added difficulty of characterizing the physical behavior of the small, often irregularly shaped fibers. Characterizations of textile materials are distinct hierarchy of structure, which should be represented by model of textile geometry and mechanical behavior. The geometric complexity of the structure and the presence of a hierarchy of structure and scale levels (10^{-5} m-fibers, 10^{-3} m-yarns/tows, 10^{-1} m-fabrics, 10^{0} m-composite parts) lead to a high complexity of the predictive models, a high level of approximation in them and to the high level of uncertainty of the predictions, when errors are accumulated from one hierarchical level to another [11]. Figure 1a shows highly magnified photographic images of twisted filament yarn structure and typical staple-spun yarn structure (ring-spun yarn). Figure 1b shows the cross section for several differing yarn structures spun from polyester fibers/filaments to similar counts and twist, and the deviations with respect to completion of the outer layers in evident [12]. Many researchers have developed modeling technique [4,8,9,10] to display the visual characteristics of real yarns as well as analytical predictive models for yarn behavior [1, 13, 14, 15, 16, 19] in field of industrial textiles. The underlying need was to be able to predict the behavior of the final structure based upon the physical behavior and mechanical properties under different applied loads of wide range of structure available. Beyond prediction, one can use the same computer tool to virtual experiments and can also produce quite realistic animations. Therefore, modeling and testing using a computer will provide great savings in terms of both manpower and time.
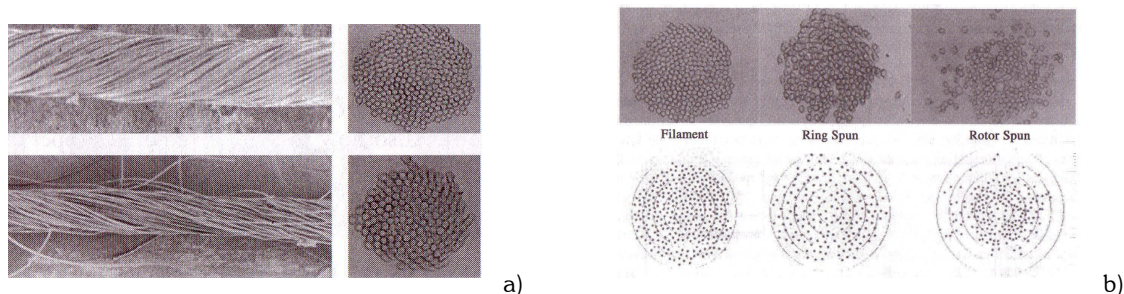

a)

b)

Fig. 1. a) Scanning electron micrograph of yarn structure; 1b) Cross section of differing yarn structure[12].

2. MODELING OF IDEAL FIBER ASSEMBLIES
2.1 Fiber Packing in Yarns Cross Section

The feature of yarn structure that can be described in a simple idealized form is the packing of fibers in yarns. Two basic forms can describe the packing of circular fibers. *Open packing*, in this form, the fibers lie in layers between successive concentric circles. In this assembly, the first layer is a single core fiber around with six fibers is arranged so that all are touching. The third layer, with has twelve fibers, is arranged so that the fibers first touch the circle that circumscribes the second layer. Additional layers are added between the successive circumscribing circles. Another idealized packing arrangement of fibers is called *close packing,* the packing of fibers of circular cross section around a single core fiber in a hexagonal configuration leads to what is call "close packing". On this form, all fibers touch each other. As the number of fibers in the cross section increases (number of layers), the yarn outline tends to become complicated and deviates from the preferred hexagonal shape. For an idea open-packed and close-packed structure, the number of fiber in each layer and the total number of fibers in the cross section are given in [6].

2.2 Geometry of Twisted Yarns

In defining the geometry of a single yarn, the model usually adopted is that of an ideal physical form. This is the coaxial-helix model illustrated in figure 2. The assumptions underlying the model are characterized by the following postulates [6, 12]:

- The yarn is circular in cross section and is uniform along its length.
- The axis of the circular cylinders coincides with the yarn axis.
- A filament at the center will follow the straight line of the yarn axis, but going out from the center the helix angle gradually increases, since the twist per unit length in all the layers remains constant.
- It is built up of a series of superimposed concentric layers of different radii in each of which the fibers follow a uniform helical path so that its distance from the center remains constant.
- The number of filaments of the fiber crossing the unit area is constant, that is the density of packing of fibers in the yarn remains constant throughout the model.
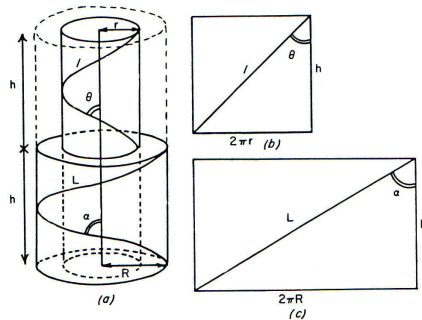

Fig. 2. a) Idealized yarn geometry and; b) "opened out" diagram of cylinder at radius r, and; c) "opened out" at yarn surface [6].

The structure is assumed to be made up of a large number of filaments; this will avoid any complications arising because of any discrepancies in packing of fibers.

3. FIBER ASSEMBLIES ALGORITHM MODEL
3.1 Outline of the Algorithm

The algorithm of 3D modeling of yarn structure has been developed. The general algorithm for fiber distribution in a yarn cross-section can now be developed by extending the algorithm D suggested by [2, 3]. The algorithm used the concept of virtual locations that are determined by the position of fibers by a distribution function in 2D that obtained the experimental results. The distributions function in the model suggested by [14] that can demonstrate all of the properties of the ideal and real yarns. A series of further cross-section at equal intervals along the yarn length is given. Each cross-section is rotated by a pre-determined amount relative to previous one, to allow for the yarn twist and parameters of fibers migration. The mathematical model of twist with variable radius suggested by[19] that can demonstrate all of the properties of the ideal and migration of fibers. The fibers curve in each interval between two successive cross-sections approximated by cubic NURBS. Also curve generation based on twist of each fiber is determined by centerline configurations of their constituent fibers and the generative model. Each fiber is created by sweeping a closed curve along a centerline path.

The algorithm requires the following input data:

i.) fiber - dimension parameters, namely, $d_f^{\max}, d_f^{\min}, d_f^{av}$ and σ_f, these being the maximum, minimum, and average diameter of fibers and mean deviation of fiber diameter, respectively.

ii.) d_y, the yarn diameter;

iii.) N_f, the number of fibers in the cross-section;

iv.) $p(R)$, the distribution for the probability that a given position within the yarn contains a fiber. This probability is taken to depend on the radial distance from the yarn axis. The distributions function used in the model shown in equation 7. The meaning of the parameters function will be discussed in detail in section 3.2.4

The proposed algorithm consists of the following steps:

i.) construct the distribution of virtual locations that takes into consideration the type of symmetry and shape of the yarn cross-section;

ii.) define those virtual locations that are occupied by fibers in accordance with the fiber-distribution probability, $p(R)$.

iii.) for all the fiber in cross-section, define the dimensions of each fiber and locate them randomly within the virtual locations determined in step ii.

iv.) Create a series of further cross-sections at equal intervals along the yarn length.

v.) Rotate each cross-section by a pre-determined amount relative to previous one, to allow for the yarn twist and parameters of fibers migration (amplitude and frequency of fiber migration). The parameters of fibers migration used in the model shown in equation 8-11. The meaning of the parameters function will be discussed in detail in section 3.3.

vi.) Curve generation base on twist of each fiber is determined by centerline configurations of their constituent fibers and the generative model to create each fiber by sweeping a closed curve along a centerline path.

3.2 Virtual Locations

3.2.1 General Model

This algorithm uses the concept of 'virtual locations' or fibers in a cross-section occupy cells. The positions of virtual locations are determined by distribution functions [2]. Each fiber in the cross-section can occupy a virtual location among the fibers surrounding it. Virtual locations can have several points of contact with their neighbors. The position of the fiber within a virtual location is random. Three types of model that use virtual locations can be considered that are 'one fiber – one location', 'one fiber – several locations and ring configuration model.
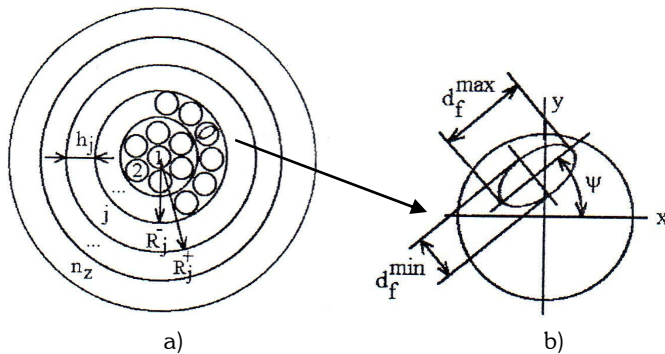

Fig. 3. The virtual-location placement for a singles yarn; a) the ring configuration of virtual location; b) the position of a fiber within a particular location [2].

The ring configuration of virtual location was used in this study that is treated as possible regions of the fiber path that may be occupied within a given cross-section. For a fiber located at a particular point in a cross-section, the number of locations in the vicinity of this fiber that contain a fiber depends upon the value of the fiber-distribution function at this point [2].

The assumed shape of the fibers in cross-sections is elliptical. The maximum and minimum dimensions of the fiber cross-section can be defined from the average diameter d_f^{av} as follows:

$$d_f^{\max} = d_f^{av} / \sqrt{\omega}$$
$$d_f^{\min} = d_f^{av} / \sqrt{\omega}$$

(1)

where $\omega = d_f^{\max} / d_f^{\min}$ is an elliptical factor characteristic of a particular fiber sample.

The random position of fiber within a virtual location can be characterized by means of the following three parameters (figure 3 a, b):

ρ_f and $\emptyset_f$, polar co-ordinates of the centre of the fiber with respect to the center of the virtual location that based on the random distribution functions in yarn cross-sections.

Ψ, the angle of tilt of the principal axis of the elliptical fiber cross-section to the axis Ox.

The parameters ρ_f and $\emptyset_f$ are in the intervals $[0, \rho_{fmax}(\rho_f)]$ and, $[0, 2\pi]$ respectively, where ρ_{fmax} corresponds to the ultimate position of the fiber within the virtual location for a given value of $\emptyset_f$. The parameter Ψ is distributed uniformly in the interval $[-\Psi_{max}, \Psi_{max}]$, where the maximum tilt $\Psi_{max}(\rho_f, \emptyset_f)$ depends on the ratio of the fiber maximum dimension $d_f^{\max}$ to the diameter of the virtual location.

3.2.2 Virtual location Model for Singles Yarns

In section 2, we introduced the ideal yarn structure. It can be assumed that the distribution of the fibers in the yarn cross-section has a rotational symmetry. It is therefore assumed that the virtual locations are ultimately densely packed into $n+1$ concentric ring zones in spite of the possible deviations of the cross-section shape from a circle. The width of each jth zone is $h_j = d_f^{av} + \sigma_f$. The center of this zone lies in the center of the fiber that is nearest to the center of gravity of all the fibers in a cross-section. The outer and inner radii of zones are, respectively, equal to [2, 3]:

$$R_j^+ = h_j j + h_j / 2; j = 0,1...,n_z;$$
$$R_0 = 0;$$
$$R_j^- = h_j(j-1) + h_j / 2; j = 1,2,....n_z.$$

(2)

The number of virtual locations within any zone does not depend upon the diameter of the virtual locations and is calculated as:

$$M_0 = 1; M_j = \text{integer}[2\pi j], j = 1,2,...n_z$$

(3)

The fiber distribution is expressed as the ratio of the number of fibers m_j in the zone j to the number of virtual locations M_j in this zone.

3.2.3 Effects of Twist in Yarn Cross-section

In order to define the properties of packing of filaments in a yarn, an index of packing fraction is used. This algorithm used the packing fraction that defined the ratio of total cross-sectional area of the yarn. In this case, it is possible to find all packing fraction results directly from scheme of cross sectional structure of yarn model [6]. The packing fraction values for each ring layer Φ_i and for the whole yarn cross-section Φ were calculated using formulas followed:

$$\Phi_i = A_{fi} / A_{yi},$$
$$\Phi = (A_{fi} + ... + A_{fi} + ... + A_{fnz})/(A_{y1} + ... + A_{yi} + ...A_{ynz}) \text{ or}$$
$$\Phi = \sum A_{fi} / \sum A_{yi}$$

(4)

where A_{fi} = total sum of cross-sectional area of all filaments in the current ring layer, A_{yi} = cross-sectional area of the current ring layer, i= current ring layer, n_z = number of the ring layers in the yarn.

If a twist is imparted to a yarn, an angle between axial line of each filament and yarn axis is not equal to zero. Therefore a crossing line of each filament in cross-section of a single twisted yarn has elliptical shape. If we assume that the filaments are inextensible during twisting, a thickness of each ring layer is equal to filament diameter d_f, that a semi-minor axis of the ellipse. A length of semi-major axis d'_f consists of its degree of slope. An equation for deriving the semi-major axis, using 'mean' inverse of cosine of inclination of filaments is

$$d'_f = d_f \overline{\sec} \beta_0$$

(5)

where β_0 = single yarn surface helix angle.

Therefore a number of filaments, which lie into the same ring layer, is less now. Consequently the number of layers in twisted yarn model is increased and, moreover, a diameter of this yarn increased. The packing fraction Φ remains in fixed level if:

$$\sum A_{fj} = (\overline{\sec} \beta_0)\sum A_{fi} \text{ and}$$

(6)

$$\sum A_{yj} = (\sec\beta_0)\sum A_{yi} \,,$$

where A_{fj}, A_{fi} = total sum of cross-sectional area of all filaments in current layer j (for twisted yarn) and in current layer i (for zero twist yarn);

A_{yj}, A_{yi} = cross-sectional area of current layer j (for twisted yarn) and current layer i (for zero twist yarn).

3.2.4 Distribution Model of Fiber in Yarn Cross-section

Initially the algorithm was applied to continuous filament yarns and circular in cross-sections with the fibers arranged entirely with this region. It can be extended to staple fibers yarns or hairiness. While it is accepted that a real yarn does not have a well-defined boundary, it is useful to apply on in the model. The number of fibers is sufficiently small so that this does not represent a sudden change.

It is observed in the real yarns, [2, 7] that the center of yarns is generally denser than the outer regions. The trend is represented in the model by introducing a distribution for the probability that a given position within the yarn contains a fiber. This probability is taken to depend on the radial distance from the yarn axis. The distribution used was [14]:

$$p(R) = (1-2\varepsilon)\left\{\frac{\exp(1)-\exp(R/R_{max})}{\exp(1)-1}\right\}^{\beta} + \varepsilon \tag{7}$$

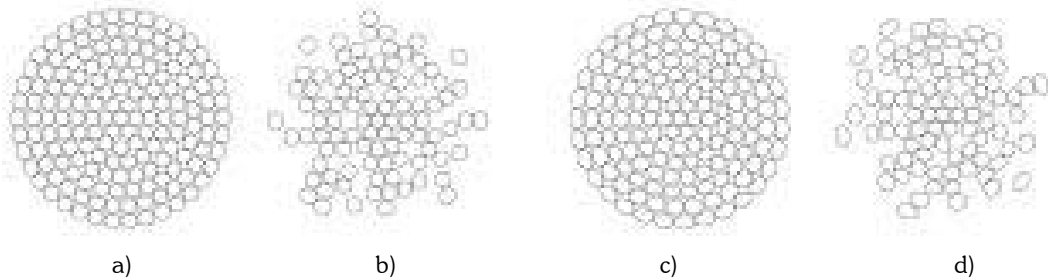where R_{max} = yarn radius, and ε, β are distribution parameters.

| a) | b) | c) | d) |

Fig. 4. example of yarns cross-sections; a) Virtual locations at 30 degree twisted angle; b) packing arrangement (ε=0.05, β= 1.2); c) Virtual locations at 45 degree twisted angle; d) packing arrangement (ε=0.05, β= 1.2).

Figure 4a, b show the example of yarns cross-sections and packing arrangement that are composed of 162 virtual locations at 30 degree twisted angle. The fibers diameter, yarn diameter and pitch are 40 μm, 0.6 mm and 3.28 mm, respectively. Also, figure 4c ,d show the example of yarns cross-sections and packing arrangement that are composed of 144 virtual locations at 40 degree twisted angle. The fibers diameter, yarn diameter and pitch are 40 μm, 0.6 mm and 1.88 mm, respectively.

In the case of ideal yarn, the β and ε parameters are equal to zero. It means that the numbers of filaments of fibers crossing the unit area are constant or the density of parking of fibers in the yarn remains constant. The typical value used guarantees that the artificial yarn boundary does not influence the behavior too much.

The β parameter controls the average packing density of the yarn and is determined from the other parameters. The packing density should be a function of the twist, while in the model these two factors are treated as independent. In the comparison with the experimental results, a simple linear relationship was applied between the two parameters. With some further investigation, a more accurate relationship may be found for a given type of fiber and spinning process.

3.3 Fiber Path of a Migrating Helix

Most of fibers in singles spun yarns do not follow the perfect coaxial helical path [12]. If a fiber is assumed to follow the path of a conical helix with maximum and minimum radii R_{max} and R_{min}, its projected radius on the x-y plane varies with the height of the helix z and the rotational angle Ø. The height of the helix is h when Ø =2π. An arbitrary point (x, y, z) on the helical fiber axis can be defined by the following:

$$x = R(\phi)\cos\phi \,, \quad y = R(\phi)\sin\phi \,, \quad z = \frac{h}{2\pi}\phi \tag{8}$$

The projected radius of the migrating helix can be defined by experimental results or by assuming certain characteristics of the yarn structure, such as the constant packing density by [5,6,18]. Therefore, the general mathematical approach developed by [19] can be applied to a wider variety of radius functions. This model assumes the projected radius of the helix has a sinuous form:

$$R(\phi) = R_{min} + \frac{R_{max} - R_{min}}{2}\left(\cos\frac{h\phi}{2\pi\lambda} + 1\right),$$

(9)

where R_{max}, R_{min} = maximum and minimum radius of the migrating helix; h = equivalent height of the migrating helix; Ø = Rotational angles; λ = wave length of migration. The difference between R_{max} and R_{min} gives the amplitude and $1/\lambda$ the frequency of fiber migration. The parameters of fiber migration can be obtained directly from measurements of the fiber trace in the yarn. The term $h/2\pi$ is treated as a constant, h= z(2π). However, the method used in this algorithm is applicable to the case where this term is a function of position. The general nature of this approach permits an experimentally defined function of the projected radius of the helix, which is closer to the reality than the previous approaches [19].
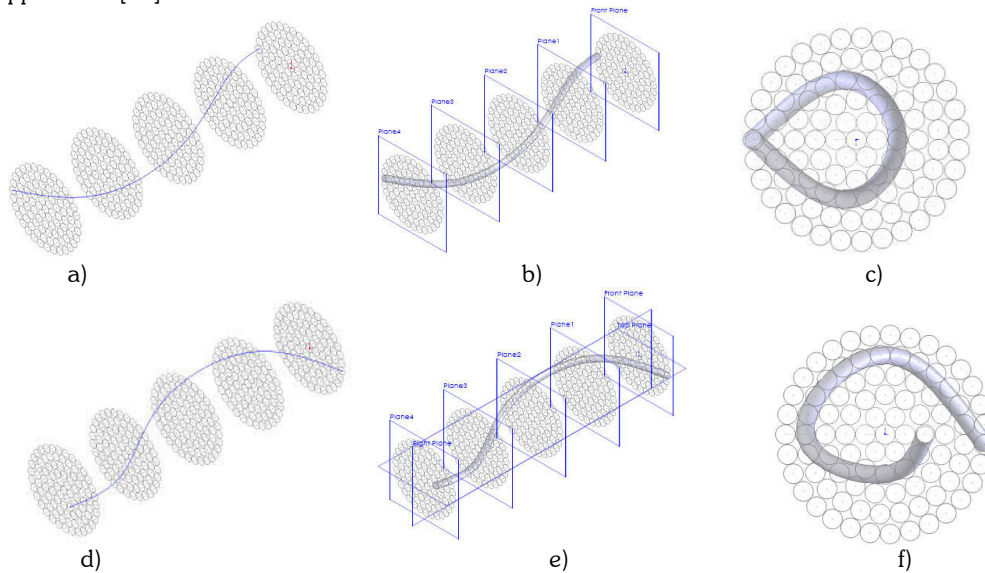

Fig. 5. the fiber migration each cross-sections; a) curve generated of migrating fiber (h/2πλ=1.0, ΔR=0.3); b) solid model of fiber migration; c) front view of solid model; d) curve generated of the first halves of migrating fiber (h/2πλ=0.5, ΔR=0.3); e) solid model of fiber migration; f) front view of solid model.

In order to compare modeling of cylindrical and migrating helices, the following geometric parameters for the migrating helix and defined to possess an equivalent relationship in both cases:
Equivalent axis length is

$$h = \frac{2\pi R_e}{\tan\theta}$$

(10)

where θ = Euler's angle. Equivalent radius R_e is defined as the mean radial position, comparable to the radius of the cylindrical helix. The migration period is $Ø_p$, and the mean radial position of the fiber is expressed as

$$R_e = \frac{1}{\phi_p}\int_0^{\phi_p} R(\phi)d\phi = \frac{R_{max} + R_{min}}{2}$$

(11)

The geometry described by equation 8 and 9 has a periodicity that can be determined by the least multiplier of the periods for cosØ (cylindrical helix) and cos(hØ/2πλ) (fiber migration). Figure 5a-f show the fiber migration each cross-sections.

3.4 Twist Curve Approximation

3.4.1 Parametric Equation

The parametric equation of the helix with radius R and pitch h is similar to that given by [20] following;

$$P(u) = [R\cos 2\pi u, R\sin 2\pi u, 2h\pi u]^T, \qquad 0 \leq u \leq 1 \tag{12}$$

The helix equation gives,

$$x = R\cos 2\pi u,$$
$$y = R\sin 2\pi u, \tag{13}$$
$$z = 2h\pi u$$

The first equation for u and substituting in the other two, we obtain the following nonparametric equation:

$$P = [x, R\sin(\cos^{-1}(x/R)), h\cos^{-1}(x/R)]^T \tag{14}$$

Solving the z component for u and substituting in the x and y equations gives the following implicit equation:

$$x - R\cos(z/h) = 0$$
$$y - R\sin(z/h) = 0 \tag{15}$$

3.4.2 NURBS Curves Approximation

In the case of fibers migration, the fiber curve in each between two successive cross-sections can be approximated by a 3D rational B-spline curve (NURBS). NURBS curves are parametric splines, whose main components are the 2D or 3D control points or control vertices, the weights of these points, and a knot vector limiting the effect of the control vertices onto a given segment of the curve. If the weights of all control vertices are similar, the NURBS becomes a NUBS (*Non-Uniform B-Spline*). The basis functions of NUBS can be defined by the Cox-deBoor recursion formula:

$$B_{i,1}^{NUBS}(t) = \begin{cases} 1, & if\ t_i \leq t < t_{i+1}, \\ 0, & otherwise, \end{cases}$$

$$B_{i,k}^{NUBS}(t) = \frac{(t-t_i)B_{i,k-1}^{NUBS}(t)}{t_{i+k-1}-t_i} + \frac{(t_{i+k}-t)B_{i+1,k-1}^{NUBS}(t)}{t_{i+k}-t_{i+1}},\ \text{if k} > 1, \tag{16}$$

where t_i is an element of the knot vector and k is the level of NUBS. Note that if the number of control vertices is n, then the number of weights is also n, but the number of knot values is $n + k - 1$, where k is the level of the curve. In the active range of the parameter domain, the NUBS basis functions sum up to 1. When we associate an additional scaling of these masses, called the weights and denoted by w_i, we can define the NURBS curve. Using the same center of mass analogy, the point on the NURBS curve for a given parameter t is obtained as:

$$\vec{r}(t) = \frac{\sum_{i=0}^{n-1} w_i B_i^{NUBS}(t).\vec{r}_i}{\sum_{j=0}^{n-1} w_j B_j^{NUBS}(t)} = \sum_{i=0}^{n-1} B_i^{NURBS}(t) \cdot \vec{r}_i, \tag{17}$$

where r_i is an element of the array of control points (n is the number of elements). The weights of CVs can be less or greater than 1.

Given data points $\{d_i\}$, and associating parameters $\{\vec{r}(t)\}$, i = 0, 1, ..., m. The approximation curve $\vec{r}(t)$ in the least squares sense is defined by [17]

$$\text{Minimize } \sum_{i=0}^{m} \left\| d_i - \vec{r}(t) \right\|^2 \tag{18}$$

The user specifies the points and wants the curve to pass this point as closely as possible.

4. CAD/CAE OF FIBER ASSEMBLIES
4.1 Computer-Aided Design of Fiber Assemblies

The SolidWorks software package was used to model the fibers assemblies. A CAD modeling approach that provides a 3 dimensional geometric representation of the yarn structure based on the algorithm. Procedure of constructing yarns structure is shown in figure 6. The figure shows the construction of four-layers fibers assemble. Each fiber diameter is 40 μm. The yarn is composed of 33 filaments, of which the diameter and pitch is 0.28 mm and 1.524 mm,

respectively. The graphical results of yarn structure are presented in figure 7. The ideal fibers assemblies of 20, 30 and 40 degree twisted angle are shown in figure 7 a-c, respectively. An average fibers diameter is 40 μm. Figure 7a shows the S twist (right-handed twist or clockwise) that there are 36 filaments at 20 degree twisted angle. Also figure 7b shows the S twist of 33 filaments at 30 degree twisted angle. Figure 7c presents the Z twist (left-handed twist or anticlockwise) that there are total 32 filaments at 40 degree twisted angle. Figure 8d-f shows the fibers assemble of z twist of fibers migrations. There are 33 filaments at 30 degree twisted angle and the parameters of fibers migration are changed to ΔR= 0.1, 0.2 and 0.4, respectively. In this modeling, we assumed that the β and ε parameters the equal to zero and the fibers are circular in the cross section. It means that the numbers of filaments of fibers crossing the unit area are constant.
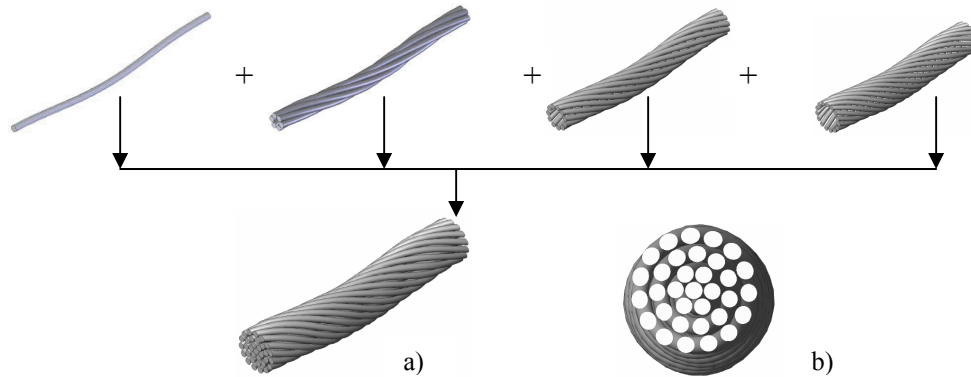

Fig. 6. a) the assemble model of each layer of yarn structure (h/2πλ=1.0, ΔR=0.4, 30 degree of twisted angle); b) front view of yarn structure.

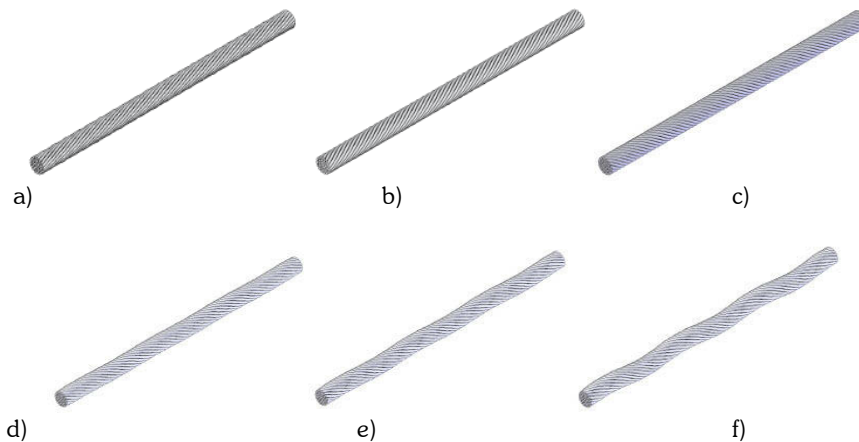Fig. 7. ideal and migration of fibers assemblies (Ø=0.28 mm, length = 5 mm); a-c) Ideal structure of yarns at 20, 30, 40 degree twisted angle; d-f) fibers migration (h/2πλ=1.0 and 30 degree twisted angle) for ΔR=0.1, 0.2 and 0.4.

4.2 Computer-Aided Engineering of Fibers Assemblies

The yarns structure model was constructed through the proposed algorithm. The geometric information and material information can directly provide each distinctive constituent in the fibers assemblies. The integration of the CAD/CAE for prediction of the yarn behavior becomes possible. The SolidWorks and COSMOSWorks software package were used to model fibers assemblies and predict the behavior of final structure based upon the physical behavior and mechanical properties under different load applied. In this study, the finite element analysis presented the mechanical properties of the fiber which are assumed to be linear elastic with either isotropic or orthotropic constitutive properties. The material properties and finite element meshes obtained from COSMOSWorks were used. In this case, nylon 101 and tetrahedral element mesh were used to simulate yarns behavior. Figure 8a presents one turn of yarn model

(Ø=0.2 mm, pitch=1.048 mm) before extension. The match meshes at the fiber to fiber interface are basic requirement in order to successfully conduct finite element analysis. The interface between the fiber to fiber are assumed to be bonded throughout the model, with compatible mesh options. Figure 8b-d show the response of three ideal yarn models, extension and compression in the axial direction and yarn bending. The extension model clearly shows the stress distribution and necking of the yarn piece, whereas the compression model opens significantly as the fibers buckle to avoid compression of the fiber material. For the yarn bending model, the cross sections of the yarn do not remain in a plane. There is a tendency for each fiber to move along its axis in the direction of the outside of the curve. Figure 9 shows the three responses of fibers migration of one turn of yarn model (Ø=0.28 mm, pitch=1.524 mm) with extension, compression and bending conditions. Also, figure 10 shows the stress distribution and deformation after compression and extension of yarn model (Ø=0.28 mm, length=5 mm and pitch=1.524 mm). The finite element analysis presented in this section is to demonstrate the stress distribution and visual images of yarn structure after load applied. Therefore, the numerical results were not compared with any real yarn property data.
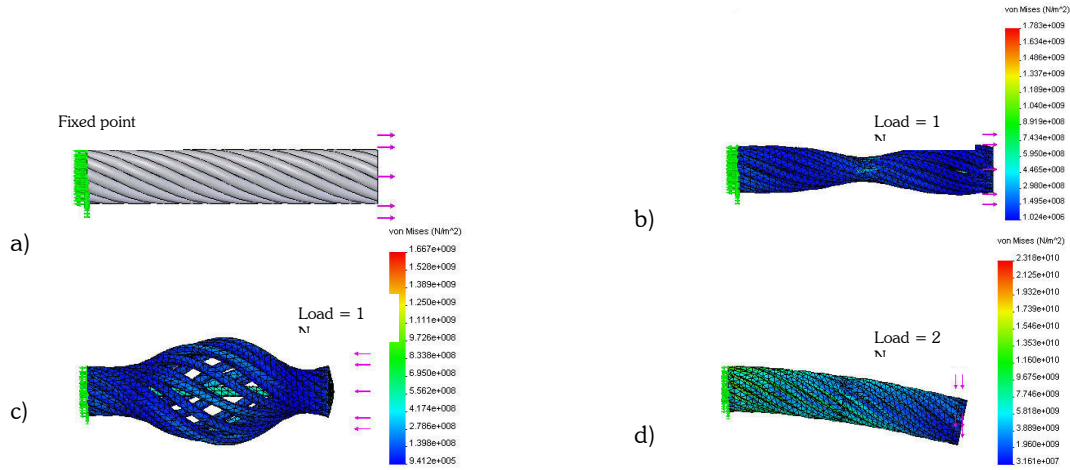

Fig. 8. The FEA for ideal yarn of 3 layers, 18 filaments at 26.6 degree of twisted angle with following conditions; a) yarn before extension; b-c) axial extension and compression of yarn model; d) bending of yarn model.
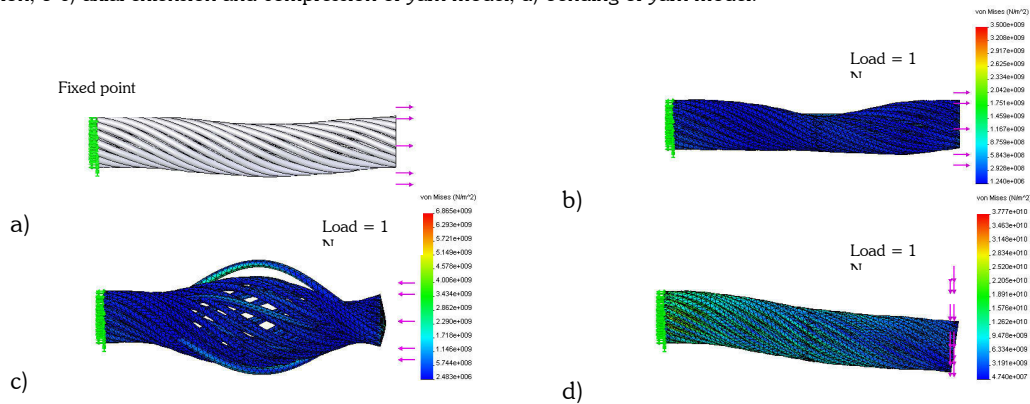

Fig. 9. The FEA for fiber migration (h/2πλ=1.0, ΔR=0.4) of 4 layers, 33 filaments at 30 degree of twisted angle; a) yarn before extension; b-c) axial extension and compression of yarn model; d) bending of yarn model.
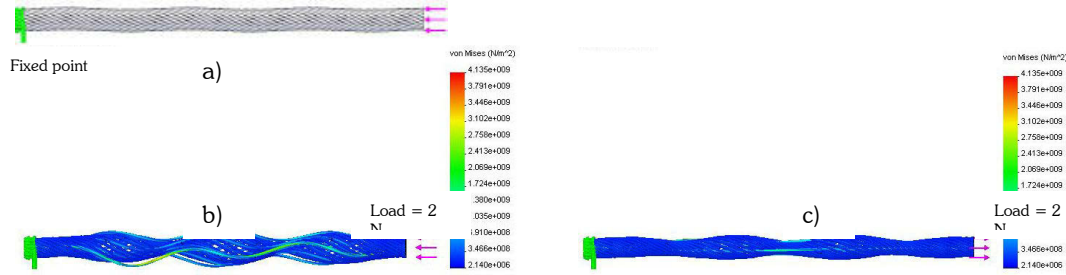
Fig. 11. The FEA of fiber migration (h/2$\pi\lambda$=1.0, ΔR=0.2) of 4 layers, 33 filaments at 30 degree of twisted angle; a) yarn before compression; b-c) stresses distribution along the axial of compression and extension of yarn model.

5. REFERENCES

[1]   Djaja, R. G., Moss, P. J, and Carr, A. J., Finite Element Modeling for an Oriented Assembly of Continuous Fibers, *Textile Research Journal*, Vol. 62, No. 8, 1992, pp 445-457.

[2]   Grishanov, S. A., Lomov, S. V., Cassidy, T. and Harwood, R. J., The Simulation of the Geometry of a two-component yarn Part II: Fibre distribution in the yarn cross-section, *Journal of textile Institute*, Vol. 88, Part 1, No. 4, 1997, pp 352-372.

[3]   Grishanov, S. A., Harwood, R. J. and Bradshaw, M. S., A model fibre migration in staple-fibre yarn, *Journal of textile Institute,* 90 Part 1, No. 3, 1999, pp 298-321.

[4]   Harwood, R. J., Liu, Z., Grishanov, S. A., Lomov, S. V. and Cassidy, T., Modelling of Two-component Yarn part II: Creation of the Visual Images of Yarns, *Journal of textile Institute,* 88 Part 1, No. 4, 1997, pp 385-399.

[5]   Hearle, j.W.S., Gupta, B. S. and Merchant, V. B., Migration of Fibers in Yarns, Part I: Characterization and Idealization of Migration behavior, *Textile Research Journal*, Vol. 35, 1965, pp 329-334.

[6]   Hearle, J. W. S., Grosberg, P. and Backer, S., *Structural Mechanics of Fibers, Yarns and Fabrics*, John Wiley &Sons, 1969.

[7]   Hickie, T. S., and Chaikin, M., Some Aspects of Worsted-Yarn Structure Part III: The Fiber-Packing Density in the Cross-Section of some Worsted Yarns, *Journal of Textile Institute*, Vol. 65, 1974, pp 443-437.

[8]   Jiang, Y and Chen, X., Geometric and algebraic algorithms for modeling yarn in woven fabrics, *Journal of Textile Institute*, Vol. 96, 2005, pp 237-245.

[9]   Keefe, M., Edwards, D. and Yang, J., Solid Modeling of Yarn and Fiber Assemblies, *Journal of the Textile Institute*, Vol. 83, No. 2, 1992, pp 185-196.

[10]   Keefe, M., Solid Modeling of Fibrous Assemblies: Part I, Twisted Yarns, *Journal of the Textile Institute*,   Vol. 85, No. 3, 1994, pp 338-349.

[11]   Lomov, S. V., Huysmans, G., Luo, Y., Parnas, R. S., Prodromou, A., Verpoest, I., and Phelan, F. R., Textile composites: modeling strategies, *Composites Part A: applied science and manufacturing,* 32, 2001, pp 1379-1394.

[12]   Lawrence, C. A., *Fundamentals of Spun Yarn Technology*, CRC Press, 2003.

[13]   Langenhove, L. A, Simulating the Mechanical Properties of a yarn Based on the Properties and Arrangement of its fibers Part I: The Finite Element Model, *Textile Research Journal*, Vol. 67, No. 4, 1997, pp 263-268.

[14]   Morris, P. J., Merkin, J. H., and Rennell, R. W., Modeling of Yarn Properties from Fiber Properties, , *Journal of Textile Institute*, Vol. 90, 1999, pp 322-335.

[15]   Munro, W. A., Carnaby, G. A., Carr, A. J. and Moss, P. J., Some Textile applications of finite-element analysis Part I: Finite elements for aligned fibre assemblies, *Journal of Textile Institute*, 88 Part 1, No.4, 1997, pp 325-338.

[16]   Munro, W. A., Carnaby, G. A., Carr, A. J. and Moss, P. J., Some Textile applications of finite-element analysis Part II: Finite elements for yarn mechanics, *Journal of Textile Institute*, 88 Part 1, No. 4, 1997, pp 339-351.

[17]   Piegl, L., and Tiller, W., *The NURBS book*, Springer-Verlag Berlin Heidelberg, 1997.

[18]   Treloar, L., A Migration Filament Theory of Yarn Properties, *Journal of Textile Institute,* Vol. 56, 1965, pp 359.

[19]   Xiaoming, T., Mechanical Propertied of a Migrating Fiber, *Textile Research Journal*, Vol. 66, No. 12, 1996, pp 754-762.

[20]   Zeid, I., *Mastering CAD/CAM*, McGraw Hill international Edition, 2005.